Delayed epidemic peak caused by infection and recovery rate fluctuations

Maxence Arutkin, Davide Faranda, Tommaso Alberti, Alexandre Vallée

Delayed epidemic peak caused by infection and recovery rate fluctuations

Cite as: Chaos **31**, 101107 (2021); https://doi.org/10.1063/5.0067625
Submitted: 18 August 2021 • Accepted: 13 September 2021 • Published Online: 26 October 2021

Maxence Arutkin, Davide Faranda, Tommaso Alberti, et al.

Delayed epidemic peak caused by infection and recovery rate fluctuations

Cite as: Chaos **31**, 101107 (2021); doi: 10.1063/5.0067625
Submitted: 18 August 2021 · Accepted: 13 September 2021 ·
Published Online: 26 October 2021

Maxence Arutkin,[1,a)] Davide Faranda,[2,3,4] Tommaso Alberti,[5] and Alexandre Vallée[6,b)]

AFFILIATIONS

[1]UMR CNRS 7083 Gulliver, ESPCI Paris, 10 rue Vauquelin, 75005 Paris, France
[2]Laboratoire des Sciences du Climat et de l'Environnement, CEA Saclay l'Orme des Merisiers, UMR 8212 CEA-CNRS-UVSQ, Université Paris-Saclay & IPSL, 91191 Gif-sur-Yvette, France
[3]London Mathematical Laboratory, 8 Margravine Gardens, London W6 8RH, United Kingdom
[4]LMD/IPSL, Ecole Normale Superieure, PSL Research University, 75005 Paris, France
[5]INAF-Istituto di Astrofisica e Planetologia Spaziali, via del Fosso del Cavaliere 100, 00133 Rome, Italy
[6]Department of Clinical Research and Innovation, Foch hospital, 92150 Suresnes, France

[a)]**Author to whom correspondence should be addressed:** maxence.arutkin@espci.fr
[b)]alexandre.g.vallee@gmail.com

ABSTRACT

Forecasting epidemic scenarios has been critical to many decision-makers in imposing various public health interventions. Despite progresses in determining the magnitude and timing of epidemics, epidemic peak time predictions for H1N1 and COVID-19 were inaccurate, with the peaks delayed with respect to predictions. Here, we show that infection and recovery rate fluctuations play a critical role in peak timing. Using a susceptible–infected–recovered model with daily fluctuations on control parameters, we show that infection counts follow a lognormal distribution at the beginning of an epidemic wave, similar to price distributions for financial assets. The epidemic peak time of the stochastic solution exhibits an inverse Gaussian probability distribution, fitting the spread of the epidemic peak times observed across Italian regions. We also show that, for a given basic reproduction number R_0, the deterministic model anticipates the peak with respect to the most probable and average peak time of the stochastic model. The epidemic peak time distribution allows one for a robust estimation of the epidemic evolution. Considering these results, we believe that the parameters' dynamical fluctuations are paramount to accurately predict the epidemic peak time and should be introduced in epidemiological models.

Dynamical stochastic models [such as the susceptible–infected–recovered (SIR) model] strongly depend on the model parameters, and uncertainty or fluctuations of these parameters propagate to long term infection count estimation. By analyzing a SIR model with fluctuating parameters, we found an analytical solution of the infection count depending on the parameter's fluctuations. Moreover, previous works have suggested that there is a delay between the epidemic peak date and its prediction using standard epidemiological models (without fluctuations). Our modeling offers a new guideline to predict the epidemic peak date, as observed for Italian regional data.

I. INTRODUCTION

To control the spread of infectious diseases, researchers have built a great deal of mathematical models to study their dynamical behaviors. The formulation of these models is based on a set of dynamical equations that represent the state of a fixed population whose individuals are split in compartments or individually modeled. Hypotheses based on clinical trials allow us to change the health status of the individuals or the relative size of compartments. Many aspects of epidemic modeling have been deeply studied, compartmental fluctuations,[1] network epidemics to incorporate the structure of the contact network that facilitates the pathogen spread and

giving birth to the GLEAM a computational framework offering real-time predictions for the pathogen spread.[2–5] More recently, agent based models were used to probe more complex interactions between people and to assess the relative benefits of various mitigation and suppression strategies aimed to control the spread of COVID-19.[6,7]

Mathematical models for epidemics are fundamental to understand the course of the epidemic and to plan effective control strategies. An important parameter is the basic reproduction number R_0, the expected number of cases directly generated by one case in a population where all individuals are susceptible to infection. This parameter is most important to understand if a pathogen can spread in the population and to predict the epidemic trajectory.[8–11] Different governments have taken many measures, such as complete lockdown, national and international travel restrictions, or mandatory quarantine, to limit the spread, but unforeseen increases within communities or regions have been observed.[12,13] Strict measures, such as quarantine, have proven to be effective in controlling COVID-19[14] and have reduced $R_0 < 1$.[15] Moreover, previous studies have shown that prediction models are characterized by several uncertainties resulting in fluctuating control parameters of the epidemics.[16–19]

A recent extensive study assessed the predictive performance of international COVID-19 forecasting models on the mortality peak and on the peak timing prediction. Although the amplitude of the mortality peak seems to be well predicted, a dispersion of the epidemic peak time (EPT) across all regions is observed, highlighting a lag between the EPT and model predictions, with an overall error across models of 20 days.[20] Similar time delays have been mentioned for the H1N1 flu, with up to two weeks delay.[2] Many hypotheses have been mentioned to explain discrepancy between the prediction and observed EPT,[21–24] but remain uncertain and worsen the situation for modeling the scenarios.

This article studies the impact of the daily fluctuations of infection and recovery rates on a susceptible–infected–recovered (SIR) model dynamic. We show that infection and recovery rate fluctuations have a major role in the peak timing. By using a SIR model with daily fluctuations, we show that an asymptotic form of the solution of the infection counts at short time is derived allowing the derivation of an analytical form of the first passage time to the epidemic peak. Moreover, for a given basic reproduction number R_0, the deterministic model anticipates the peak with respect to the most probable and average peak time of the stochastic model. This analytical result is confronted to numerical simulations and a data analysis is performed on Italian regions to illustrate our findings.

II. FLUCTUATION IMPACT ON SIR DYNAMICS

A widely used epidemiological model is the SIR model belonging to the class of compartmental models.[25] This compartmental model divides the population into three groups, namely, susceptible (S), infected (I), and recovered (R) individuals, according to the discrete-time evolution equations defined in the supplementary material. Its parameters are the recovery rate (β) and the infection rate (λ). Without fluctuations, the infection counts exhibit an exponential growth behavior, i.e., if $\lambda \leq \beta$ or $R_0 = \frac{\lambda}{\beta} \leq 1$, there is no epidemic outbreak; this is called the epidemic threshold and highlights the importance of R_0 to understand and control an epidemic dynamic.[1,9,11,26] A SIR model[16] with time-dependent control parameters can mimic the dependence of additional/external factors such as variability in the detected cases, different physiological response to the virus, release, or reinforcement of distancing measures.[17] In order to consider time-dependent control parameters, a stochastic approach is used through which the control parameters $\kappa \in \{\beta, \lambda\}$ are described by a stochastic process as follows:

$$\kappa_t = \kappa_0(1 + \sigma_\kappa \epsilon_{\kappa,t}), \tag{1}$$

where ϵ is a reduced centered Gaussian random variable. $\kappa_0 \in \{\beta_0, \lambda_0\}$ is set to be the mean value of the parameter. The numerical experiments are performed by discretizing a SIR model defined in the supplementary material with an Euler scheme and a time step $\Delta t = 1$ day following the guideline defined by Faranda and Alberti.[17] To provide an idea of the risk of observing uncontrolled epidemic growth even with $R_0 < 1$, we show in Fig. 1 an ensemble of 1000 realizations of the stochastic SIR model with $R_0 = 0.97$ and normally distributed noise of standard deviations $\sigma_\lambda = \sigma_\beta = 0.2$. Results are displayed in terms of $C(t)$, the cumulative number of

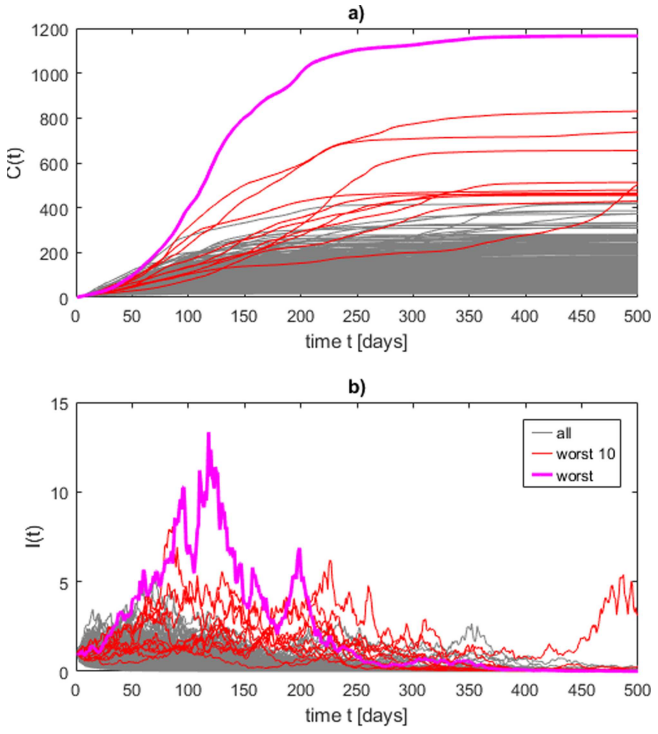

FIG. 1. Examples of COVID-19 trajectories of a stochastic SIR model. 1000 COVID-19 epidemic trajectories realized in the stochastic SIR with $I_{t=0} = 1$, $N = 10^5$, $t = 0, 1, \ldots, 500$, $\beta_0 = 0.3731$, $\sigma_\beta = 0.2$, $R_0 = 0.97$, $\lambda_0 = R_0\beta_0$, and $\sigma_\lambda = 0.2$. (a) Cumulative infections $C(t) = \sum_{i=0}^{t} I(t)$ and (b) instantaneous number of infections $I(t)$. The trajectory leading to the worst epidemic scenarios [max $C(t)$] is in magenta, and the ten worst trajectories are in red.

infections $C(t) = \sum_{i=0}^{t} I(t)$, and $I(t)$ in panels (a) and (b), respectively. Despite the average $R_0 < 1$, we observe growing epidemic phases in almost all the trajectories and some remarkable cases (highlighted by magenta and red lines), which could be identified as an epidemic concerning scenario.

A. Asymptotic solution of the stochastic infection counts

At the beginning of the epidemic, the number of susceptible people in this phase is considered constant ($S \sim N = \text{constant}$) and large with respect to the number of infected people; we can solve the discrete Euler scheme as a geometric series. Without additional assumptions, the number of infected people at a time step t reads

$$I(t) = I_0 \prod_{i=1}^{t} (1 + m + \tilde{\sigma}\epsilon_i), \tag{2}$$

with $m = \lambda_0 - \beta_0$, $\tilde{\sigma} = \sqrt{\beta_0^2\sigma_\beta^2 + \lambda_0^2\sigma_\lambda^2}$ and ϵ_i independent reduced centered Gaussian random variables. A probability distribution is fully characterized by its moments; therefore, we compute the kth

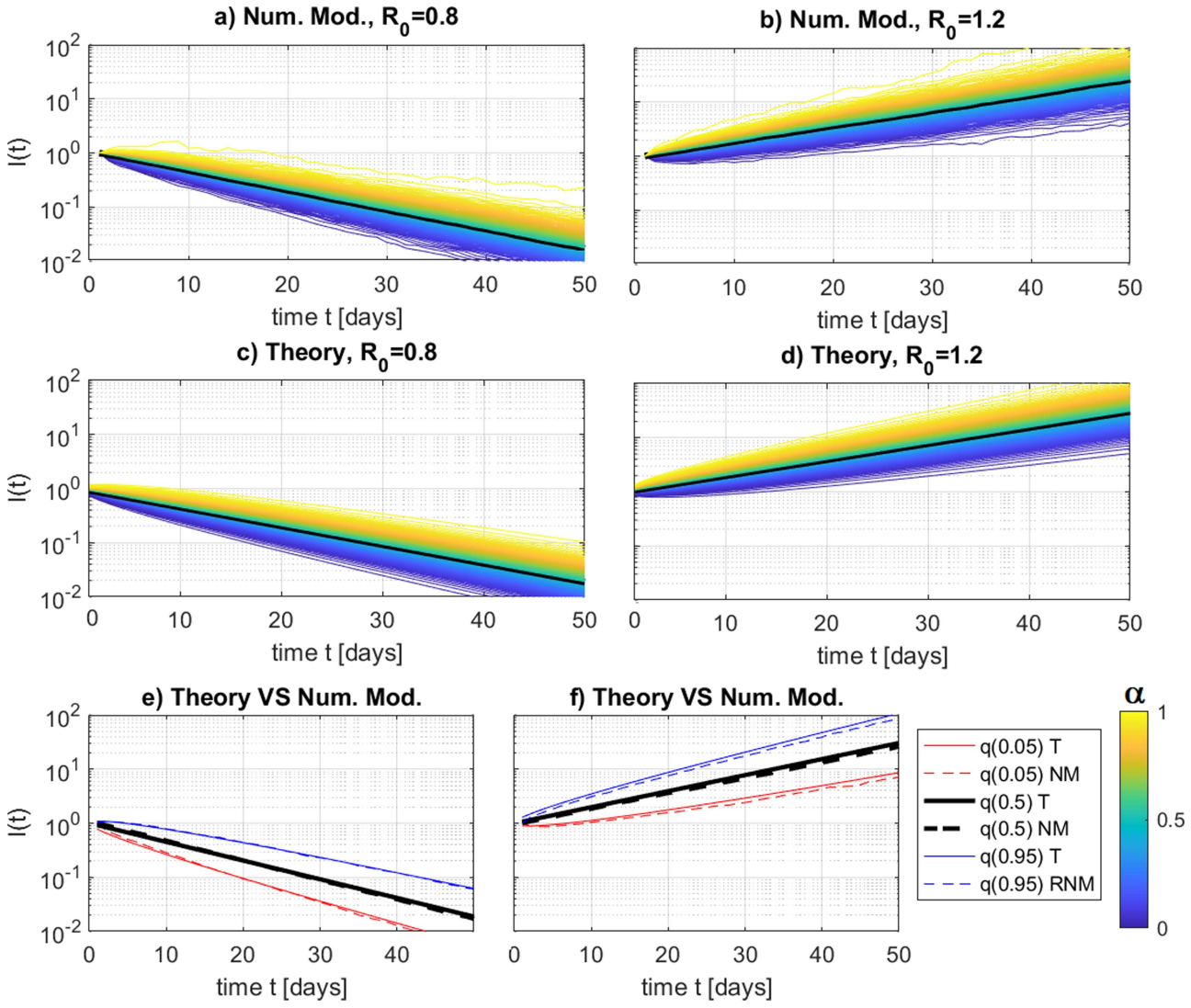

FIG. 2. Numerical and theoretical quantiles of the stochastic SIR model solution. Numerical [(a) and (b)] and theoretical [(c) and (d)] solutions of the stochastic SIR model in terms of $I_\alpha(t)$ computed with the same parameters described in the first figure of the article but $R_0 = 0.8$ [(a), (c), and (e)] and $R_0 = 1.2$ [(b), (d), and (f)]. Color-scales in panels (a)–(d) refer to the value α, while black lines to the medians $\alpha = 0.5$. Panels (e) and (f) compare numerical (NM, dotted solutions) and theoretical (T, continuous lines) solutions for specific quantiles (see legend).

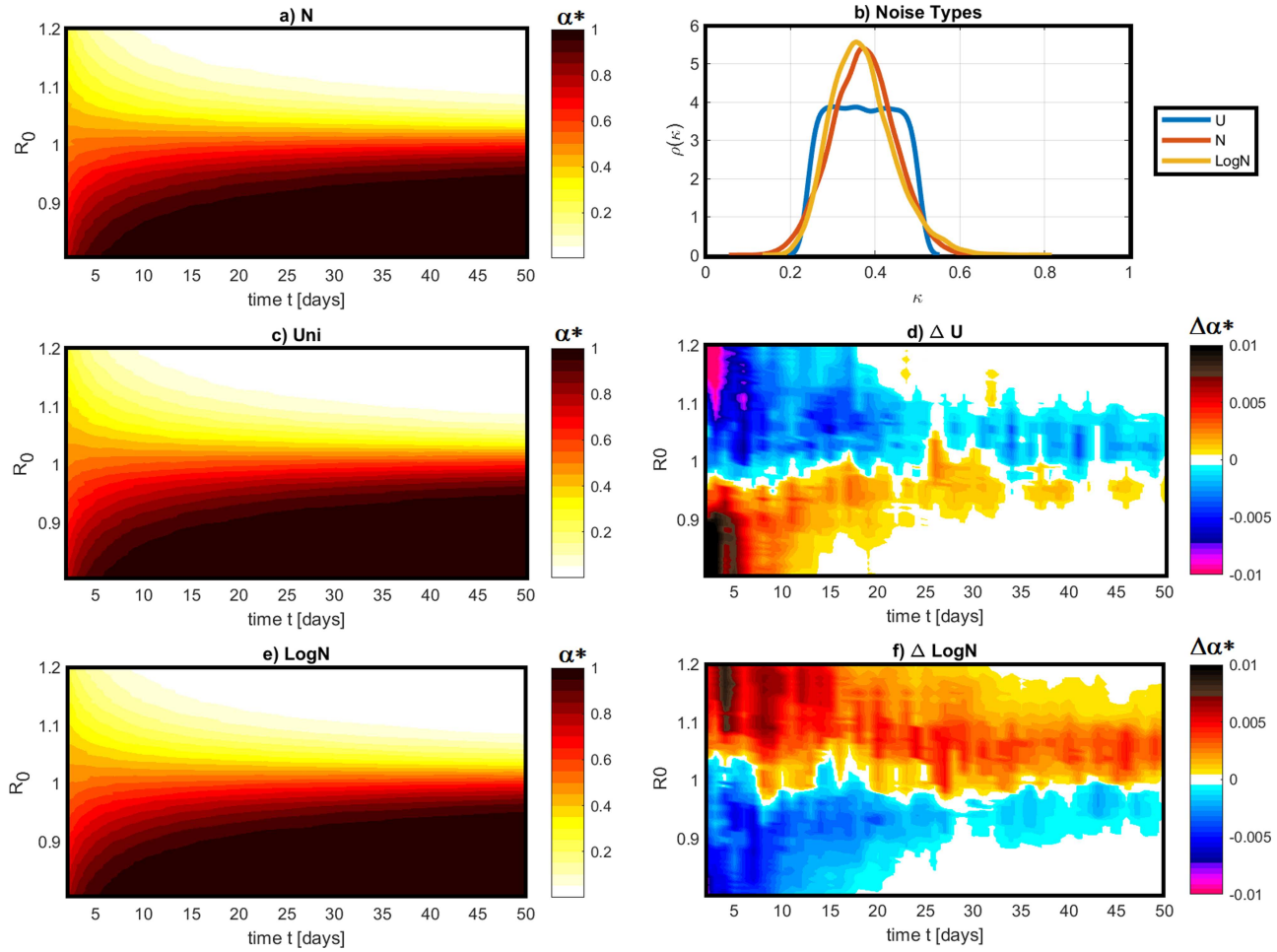

FIG. 3. Control of stochastic SIR models having different noise distributions. Panels (a), (c), and (d) show the lowest quantile α^* leading to epidemic growth phases $\alpha^* = \min(\alpha : I_\alpha(t) > 1)$, for the different noise distributions described in panel (b). N for normal distribution (a) and U for the uniform (c) and (e) for a lognormal distribution having same median and standard deviation. Panels (d) and (f) show the difference in $\alpha*$ between the normal and the uniform (d) or the lognormal (f).

moment of the solution $\forall k \in \mathbb{N}_+^*$,

$$\mathbb{E}\left[\left(\frac{I(t)}{I_0}\right)^k\right] = \prod_{i=1}^{t} \mathbb{E}\left[(1+m+\tilde{\sigma}\epsilon_i)^k\right] \tag{3}$$

$$= \mathbb{E}\left[(1+m+\tilde{\sigma}\epsilon)^k\right]^t, \tag{4}$$

and using Newton's binomial, one can find

$$\mathbf{E}\left[(1+m+\tilde{\sigma}\epsilon)^k\right] = \sum_{j=0}^{k} \binom{k}{j} (1+m)^{k-j}\tilde{\sigma}^j \mathbf{E}\left[\epsilon^j\right], \tag{5}$$

if ϵ is a reduced centered Gaussian random variable, therefore, its moments verify $\mathbb{E}\left[\epsilon^j\right] = \frac{j!}{2^{j/2}(j/2)!}$ if j is odd, zero otherwise. Thus, in the limit of small fluctuation, the kth moment of the solution reads

$$\mathbb{E}\left[\left(\frac{I(t)}{I_0}\right)^k\right] \sim \exp\left(\left(m - \frac{\tilde{\sigma}^2}{2(1+m)^2}\right)kt + \frac{\tilde{\sigma}^2}{2(1+m)^2}k^2 t\right), \tag{6}$$

where the form of the kth moment of the solution is exactly a lognormal distribution. Interestingly, the number of infected people follow the same dynamic as the price of a financial asset, a lognormal distribution with a drift;[27,28] in the price stochastic differential equation,[29] the drift of the analogous asset would be m and its volatility $\frac{\tilde{\sigma}}{(1+m)}$. At the early stage, the number of infected people is described by the following distribution:

$$I_t = I_0 \exp\left(\left(m - \frac{\tilde{\sigma}^2}{2(1+m)^2}\right)t + \frac{\tilde{\sigma}}{(1+m)}W_t\right), \tag{7}$$

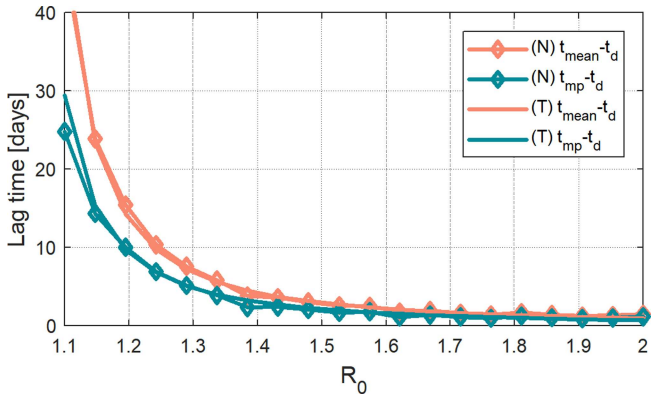

FIG. 4. Epidemic peak delay due to control parameters fluctuation. Lag time between expected EPT t_{mean} and the deterministic EPT (t_d) (orange) and most probable EPT $t_{mp} - t_d$ (dark green), computed numerically (N, diamonds) with the SIR model with conditions specified in equations in the supplementary material and $1.1 < R_0 < 2$ and from the analytical predictions (T, continuous lines). Analytical predictions are approximated for the exponential phases, whereas at the epidemic peak, the solution is no longer exponential.

with W_t being the Brownian motion. One can easily check that the average of the solution Eq. (7) follows the exponential growth expected from a deterministic SIR model. Figure 2 shows a comparison between the theoretical and numerical solutions for two cases $R_0 = 0.8$ and $R_0 = 1.2$.

B. Quantile of the stochastic solution

An analytical form I_α of the quantiles of the solution for a given confidence level α is derived in the supplementary material. Figure 3 shows the control of stochastic SIR models having different noise distributions. Panels (a), (c), and (d) show the lowest quantile α^* leading to epidemic growth phases $\alpha^* = \min(\alpha : I_\alpha(t) > 1)$, for the different noise distributions described in panel (b). Despite different noise distributions, results are similar and show only differences of quantiles of the order of 1%. This reinforces the idea that our findings are rather independent of higher order moments of the noise distributions of the parameters provided that we can fix medians and standard deviations.

C. Epidemic peak time seen as a first passage event

A time of major importance in the epidemic control is the EPT, where it can be seen as the maximum of the stochastic SIR trajectory. From a modeling point of view, we can derive an analytical formula for the EPT distribution using the following approximation: we assume that the EPT is the first passage time of the drifted lognormal distribution to the deterministic peak level, see equations in the supplementary material for full probability distribution; the average EPT t_{mean} and the most probable EPT t_{mp} are also derived analytically. Figure 4 shows the epidemic peak delay due to control parameters fluctuation. Lag times $t_{mean} - t_d$ (dark green) and $t_{mp} - t_d$ (orange) are computed numerically (N, diamonds) with the SIR model (with conditions specified in equations in the supplementary material and $1.1 < R_0 < 2$) and from the analytical

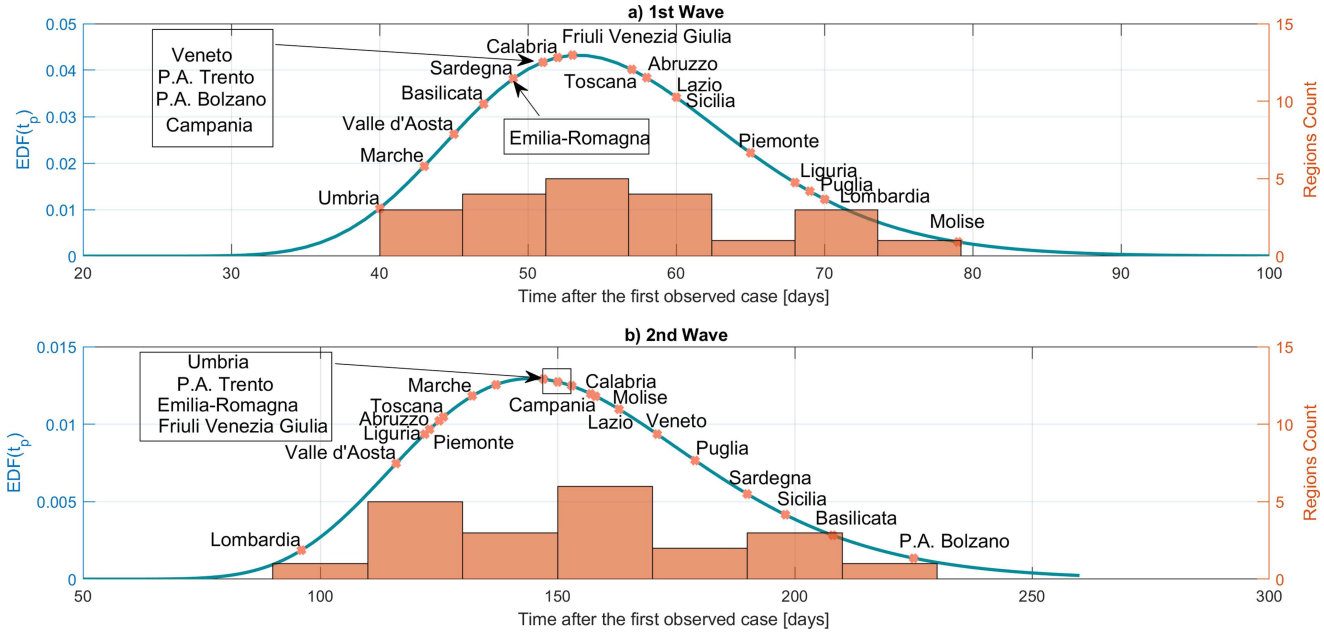

FIG. 5. Epidemic peak time distribution. Epidemic peak time computed starting from the time after the first observed case (a) and after the minimum of infection counts between first and second wave (b). The empirical distribution function (EDF) of the epidemic peak is displayed in continuous azure lines, and an histogram of the region counts by the peak date is shown in orange.

predictions (T, continuous lines). Analytical predictions are approximated for the exponential phases, although at the epidemic peak the solution is no longer exponential. Nonetheless, this approximation well predicts the lag between the deterministic and the stochastic EPT. To compare this with real data, we consider the Italian regional infection counts collected by the Italian Protezione Civile (https://github.com/pcm-dpc/COVID-19) and report the EPT distribution in Fig. 5. For each region, the first epidemic wave started after the first observed case (a). For the second wave (b), we took the day with the lowest number of infections between the first wave to the second peak. The empirical distribution function (EDF) of the EPT for the first and the second wave is fitted using maximum likelihood estimates of the theoretical EPT distribution defined in equations in the equations in the supplementary material; we assumed in this analysis that each region has the same population, 2×10^6 people, the average population of the Italian regions. A histogram of the region counts by the peak date is also presented. The large spread of the EPT is compatible with the theoretical findings.

III. DISCUSSION

Understanding the short-term prediction in the early stage of the evolution of key pandemic indicators remains a major goal for policy-makers and health professionals. The trajectory forecast of COVID-19 pandemic depends on four stages: (a) virus attributes itself (with transmissibility of the variant involved), (b) location characteristics with population density and transport use, (c) individual behaviors face to pandemic, and (d) government actions.[20–24,30] These behavioral responses are associated with a more linear growth of epidemics,[23,31] but still a few remain used in the dynamic modeling of SARS-CoV-2 transmission.

Then, it appears essential to take into account fluctuations in the modeling of the pandemic spread from the early stages to better predict the epidemic peak. However, accurately assessing the scenario that looms at the beginning of the epidemic remains an extremely complicated task. The validity of such claims depends on the evidence to support the hypotheses regarding the impact of a policy on transmission.[20] It has been shown that the gross scale of the epidemic can be understood and estimated on the basis of its distinguished dynamics. The possible trajectories of an outbreak depend on levels of public health interventions such as quarantine and precautionary measures.[32] Uncertainty in peak and date sizes can be due to many factors, including heterogeneity of contact profiles, spatial variation, and dynamics of epidemiological parameters that introduce stochasticity in the early dynamics.[33]

The prediction of R_0 is a great challenge with important practical implications because it will help support governments to quickly develop strategies to avoid any harmful conditions. Our findings provide policy-makers with a tool to assess the consequences of the possible fluctuations in policy strategies on different R_0 levels. The simulations suggest that strong social-distancing measures are needed, but fluctuations in these measures could be associated with reinforcement in peaks of COVID-19 epidemics over short periods. Subsequent waves can occur by changing social behavior measures due to pandemic variations in imposed mitigations.[34]

We observed peaks across the Italian regions (Fig. 5); for large R_0 during the first wave, the peak is distributed around 55 days (most probable peak date), between 42 and 80 days. For the second wave at a lower R_0, the peak dates are distributed around 130 days on a much wider distribution as predicted by our theoretical and numerical models. The delayed peaks are genuine results that originate from the initial conditions of the COVID-19 pandemic and show the importance of the fluctuations in the model. Previous studies hypothesized that the exponential curve in France for H1N1 in 2009 was stopped by holidays.[2,35] Other models have shown six-week errors for cumulative death below 10%,[20] a median absolute percentage error at 10 weeks of forecasting COVID-19 resurgence for the Institute for Health Metrics and Evaluation (IHME) SEIR model,[36] and 20 days before the epidemic peak in influenza infection,[37] highlighting the importance of adequate mathematical models for forecasting pandemic peak to provide accurate health policies.

In our study, the non-trivial effect has been found on the EPT due to parameter fluctuations, and for a given basic reproduction number R_0, the deterministic model predicts a peak before the most probable and average peak date of the stochastic solution. Furthermore, the predicted lag diverges when $R_0 \to 1$. The use of R_0 calculation estimates for public health policy-making is based on the assumption that R_0 values at the beginning of the epidemic reflect the properties of the population and predict the potential rate of spread of the disease in the event of a resurgence of the epidemic.[38]

Many point peaks have been observed and have shown that hesitant or even fluctuating public health policies allow, admittedly, to lower $R_0 < 1$ but do not completely contain viral spread.[39] These resurgences over short periods of time and fading on their own may reflect viral spread even in the presence of $R_0 < 1$. Until herd immunity is not reached, the full recovery of all economic activity could lead to further waves of COVID-19 pandemic. Strict control of viral spread must be maintained in order to contain low levels of transmission. Although a temporary resurgence may be observed due to the stochasticity of the transmission dynamics, the objective of $R_0 < 1$ must be set in combination with clear and non-fluctuating public health policies to ensure the eventual extinction or at least the continuous suppression of the disease.[40,41]

IV. CONCLUSION

To summarize, we found that at the early stage, the number of infected people follows a lognormal distribution analogous to the price dynamic of a financial asset. Analyzing the EPT across Italian regions, we found a spread distribution that is explained by the first passage time to the epidemic peak of the stochastic SIR solution. This distribution has been observed by numerical simulations, and we have proposed an analytical solution for the EPT distribution based on the first passage time of the lognormal solution at the early stage. The findings suggest that the epidemic peak time depends not only on the mean value of the infection and recovery rate but also on their fluctuations. Neglecting these fluctuations could lead to inaccurate epidemic scenarios and unsuitable mitigation policies.

SUPPLEMENTARY MATERIAL

See the supplementary material for the analytical derivation of the quantile analysis and first passage time modeling of the epidemic peak. A SIR MATLAB script is provided.

ACKNOWLEDGMENTS

M.A. acknowledges discussion with Romain Paserot and Ulysse Mizrahi.

AUTHOR DECLARATIONS

Conflict of interests

The authors declare no competing interests.

Author Contributions

M.A. conceived the study and formulated and derived the models. M.A. and D.F. implemented the models. M.A., D.F., and T.A. performed the data analyses and the numerical simulations. M.A., D.F., T.A., and A.V. analyzed the results. M.A. and A.V. drafted the article. All authors contributed to and approved the final version of the article.

DATA AVAILABILITY

The data that support the findings of this study are openly available in GitHub at https://github.com/pcm-dpc/COVID-19, Ref. 42.

REFERENCES

[1]N. T. Bailey *et al.*, *The Mathematical Theory of Infectious Diseases and its Applications* (Charles Griffin & Company Ltd, 1975).
[2]M. Tizzoni, P. Bajardi, C. Poletto, J. J. Ramasco, D. Balcan, B. Gonçalves, N. Perra, V. Colizza, and A. Vespignani, "Real-time numerical forecast of global epidemic spreading: Case study of 2009 A/H1N1pdm," BMC Med. **10**, 1 (2012).
[3]P. Bajardi, C. Poletto, J. J. Ramasco, M. Tizzoni, V. Colizza, and A. Vespignani, "Human mobility networks, travel restrictions, and the global spread of 2009 H1N1 pandemic," PLoS ONE **6**, e16591 (2011).
[4]A.-L. Barabási, "Network science," Philos. Trans. R. Soc. A **371**, 20120375 (2013).
[5]A. Barrat, M. Barthelemy, and A. Vespignani, *Dynamical Processes on Complex Networks* (Cambridge University Press, 2008).
[6]R. J. Rockett, A. Arnott, C. Lam, R. Sadsad, V. Timms, K.-A. Gray, J.-S. Eden, S. Chang, M. Gall, J. Draper *et al.*, "Revealing COVID-19 transmission in Australia by SARS-CoV-2 genome sequencing and agent-based modeling," Nat. Med. **26**, 1398 (2020).
[7]S. L. Chang, N. Harding, C. Zachreson, O. M. Cliff, and M. Prokopenko, "Modelling transmission and control of the COVID-19 pandemic in Australia," Nat. Commun. **11**, 1 (2020).
[8]F. Brauer, C. Castillo-Chavez, and C. Castillo-Chavez, *Mathematical Models in Population Biology and Epidemiology* (Springer, 2012), Vol. 2.
[9]K. Dietz, "The estimation of the basic reproduction number for infectious diseases," Stat. Methods Med. Res. **2**, 23 (1993).
[10]R. M. Anderson and R. M. May, *Infectious Diseases of Humans: Dynamics and Control* (Oxford University Press, 1992).
[11]T. Obadia, R. Haneef, and P.-Y. Boëlle, "The R0 package: A toolbox to estimate reproduction numbers for epidemic outbreaks," BMC Med. Inform. Decis. Mak. **12**, 1 (2012).
[12]L. Di Domenico, C. E. Sabbatini, G. Pullano, D. Lévy-Bruhl, and V. Colizza, "Impact of January 2021 curfew measures on SARS-CoV-2 B.1.1.7 circulation in France," Eurosurveillance **26**, 2100272 (2021).
[13]P. Lemey, N. Ruktanonchai, S. Hong, V. Colizza, C. Poletto, F. Van den Broeck, M. Gill, X. Ji, A. Levasseur, A. Sadilek *et al.*, ""SARS-CoV-2 European resurgence foretold: Interplay of introductions and persistence by leveraging genomic and mobility data," Res. Sq. (published online) (2021).
[14]B. Nussbaumer-Streit, V. Mayr, A. I. Dobrescu, A. Chapman, E. Persad, I. Klerings, G. Wagner, U. Siebert, D. Ledinger, C. Zachariah *et al.*, "Quarantine alone or in combination with other public health measures to control COVID-19: A rapid review," Cochrane Database Syst. Rev. **8**(4), CD013574 (2020).
[15]B. Yang, A. T. Huang, B. Garcia-Carreras, W. E. Hart, A. Staid, M. D. Hitchings, E. C. Lee, C. J. Howe, K. H. Grantz, A. Wesolowksi *et al.*, "Effect of specific non-pharmaceutical intervention policies on SARS-CoV-2 transmission in the counties of the United States," Nat. Commun. **12**, 1 (2021).
[16]D. Faranda, I. P. Castillo, O. Hulme, A. Jezequel, J. S. W. Lamb, Y. Sato, and E. L. Thompson, "Asymptotic estimates of SARS-CoV-2 infection counts and their sensitivity to stochastic perturbation," Chaos **30**, 051107 (2020).
[17]D. Faranda and T. Alberti, "Modeling the second wave of COVID-19 infections in France and Italy via a stochastic SEIR model," Chaos **30**, 111101 (2020), arXiv:2006.05081 [q-bio.PE].
[18]T. Alberti and D. Faranda, "On the uncertainty of real-time predictions of epidemic growths: A COVID-19 case study for China and Italy," Commun. Nonlinear Sci. Numerical Simul. **90**, 105372 (2020).
[19]D. Faranda, T. Alberti, M. Arutkin, V. Lembo, and V. Lucarini, "Interrupting vaccination policies can greatly spread SARS-CoV-2 and enhance mortality from COVID-19 disease: The Astrazeneca case for France and Italy," Chaos **31**, 041105 (2021).
[20]J. Friedman, P. Liu, C. E. Troeger, A. Carter, R. C. Reiner, R. M. Barber, J. Collins, S. S. Lim, D. M. Pigott, T. Vos *et al.*, "Predictive performance of international COVID-19 mortality forecasting models," Nat. Commun. **12**, 1 (2021).
[21]G. Pullano, L. Di Domenico, C. E. Sabbatini, E. Valdano, C. Turbelin, M. Debin, C. Guerrisi, C. Kengne-Kuetche, C. Souty, T. Hanslik *et al.*, "Underdetection of cases of COVID-19 in France threatens epidemic control," Nature **590**, 134 (2021).
[22]Y. Ma, S. Pei, J. Shaman, R. Dubrow, and K. Chen, "Role of meteorological factors in the transmission of SARS-CoV-2 in the United States," Nat. Commun. **12**, 1 (2021).
[23]V. A. Karatayev, M. Anand, and C. T. Bauch, "Local lockdowns outperform global lockdown on the far side of the COVID-19 epidemic curve," Proc. Natl. Acad. Sci. U.S.A. **117**, 24575 (2020).
[24]E. B. Hodcroft, M. Zuber, S. Nadeau, T. G. Vaughan, K. H. Crawford, C. L. Althaus, M. L. Reichmuth, J. E. Bowen, A. C. Walls, D. Corti *et al.*, "Spread of a SARS-CoV-2 variant through Europe in the summer of 2020," Nature **595**(7869), 707–712 (2021).
[25]F. Brauer, "Compartmental models in epidemiology," in *Mathematical Epidemiology* (Springer, 2008), pp. 19–79.
[26]R. M. Anderson, H. Heesterbeek, D. Klinkenberg, and T. D. Hollingsworth, "How will country-based mitigation measures influence the course of the COVID-19 epidemic?," Lancet **395**, 931 (2020).
[27]L. Bachelier, "Théorie de la spéculation," Ann. Sci. Ec. Norm. Super. **17**, 21–86 (1900).
[28]J.-P. Bouchaud and M. Potters, *Theory of Financial Risks* (Cambridge, 2003), Vol. 4.
[29]J. C. Hull, *Options Futures and Other Derivatives* (Pearson Education India, 2003).
[30]J. Riou and C. L. Althaus, "Pattern of early human-to-human transmission of Wuhan 2019 novel coronavirus (2019-nCoV), December 2019 to January 2020," Eurosurveillance **25**, 2000058 (2020).
[31]P. C. Jentsch, M. Anand, and C. T. Bauch, "Prioritising COVID-19 vaccination in changing social and epidemiological landscapes: A mathematical modelling study," Lancet Infect. Dis. **21**(8), 1097–1106 (2021).
[32]H. Nishiura, K. Patanarapelert, M. Sriprom, W. Sarakorn, S. Sriyab, and I. M. Tang, "Modelling potential responses to severe acute respiratory syndrome in Japan: The role of initial attack size, precaution, and quarantine," J. Epidemiol. Community Health **58**, 186 (2004).
[33]T. D. Hollingsworth, D. Klinkenberg, H. Heesterbeek, and R. Anderson, "Mitigation strategies for pandemic influenza A: balancing conflicting policy objectives," PLoS Comput. Biol. **10**;7(2), e1001076 (2011).

[34]A. V. Tkachenko, S. Maslov, A. Elbanna, G. N. Wong, Z. J. Weiner, and N. Goldenfeld, "Time-dependent heterogeneity leads to transient suppression of the COVID-19 epidemic, not herd immunity," Proc. Nat. Acad. Sci. U.S.A. **118**, e2015972118 (2021).
[35]S. Cauchemez, A.-J. Valleron, P.-Y. Boelle, A. Flahault, and N. M. Ferguson, "Estimating the impact of school closure on influenza transmission from sentinel data," Nature **452**, 750 (2008).
[36]I. Covid, "Modeling COVID-19 scenarios for the United States," Nat. Med. **27**, 94 (2021).
[37]Q.-H. Liu, M. Ajelli, A. Aleta, S. Merler, Y. Moreno, and A. Vespignani, "Measurability of the epidemic reproduction number in data-driven contact networks," Proc. Nat. Acad. Sci. U.S.A. **115**, 12680 (2018).
[38]L. Di Domenico, G. Pullano, C. E. Sabbatini, P.-Y. Boëlle, and V. Colizza, "Impact of lockdown on COVID-19 epidemic in Île-de-France and possible exit strategies," BMC Med. **18**, 1 (2020).
[39]Y. Li, H. Campbell, D. Kulkarni, A. Harpur, M. Nundy, X. Wang, H. Nair, andUsher Network for COVID-19 Evidence Reviews (UNCOVER) Group, "The temporal association of introducing and lifting non-pharmaceutical interventions with the time-varying reproduction number (*R*) of SARS-CoV-2: A modelling study across 131 countries," Lancet Infect. Dis. **21**, 193 (2021).
[40]M. A. Rowland, T. M. Swannack, M. L. Mayo, M. Parno, M. Farthing, I. Dettwiller, G. George, W. England, M. Reif, J. Cegan *et al.*, "Covid-19 infection data encode a dynamic reproduction number in response to policy decisions with secondary wave implications," Sci. Rep. **11**, 1 (2021).
[41]J. A. Jacquez and P. O'Neill, "Reproduction numbers and thresholds in stochastic epidemic models I. Homogeneous populations," Math. Biosci. **107**, 161 (1991).
[42]J. A. Jacquez and P. O'Neill (2020) GitHub. https://github.com/pcm-dpc/COVID-19.